J. Plasma Phys. (2024), *vol*. 90, 975900601
Published by Cambridge University Press

doi:10.1017/S0022377824001454

Plasma rotation induced by biasing in axially symmetric mirrors

Alexei D. Beklemishev [1,2,†]

[1]Institute of Nuclear Physics, 11, Acad. Lavrentieva Pr., Novosibirsk, Russia, 630090

[2]Novosibirsk State University, 1, Pirogova str., Novosibirsk, Russia, 630090

(Received 16 August 2024; revised 21 October 2024; accepted 22 October 2024)

Physics of the plasma rotation driven by biasing in linear traps is analysed for two limiting cases. The first, relevant for traps with low effective viscosity, considers the line-tying effects to be responsible for the drive as well as for the dissipation of the angular momentum. Meanwhile, in long and thin traps with collisional plasma or developed turbulence, the radial transport of the angular momentum becomes its primary loss channel. The momentum flux goes into the scrape-off layer, which makes conditions there partially responsible for the achievable rotation limits.

Keywords: plasma flows, plasma devices

1. Introduction

Plasma rotation in crossed fields is present in most mirror traps; it is both the naturally occurring phenomenon and a means in which to influence the quality of confinement. Rotation is an important factor influencing axial confinement (through the plasma potential), stability of discharges and turbulent transport processes. In extreme cases (in centrifugal traps), fast rotation can also alter the equilibrium of radial forces. Rotation can be induced by many different factors, such as the radial distribution of the ambipolar potential, biasing of plasma-facing electrodes, injection of angular momentum with neutral beams, or the asymmetric confinement of particles. In equilibrium, the net sources should be exactly balanced by sinks. The loss of the angular momentum can also be due to multiple causes, the most prominent of these are the line-tying and collisional or turbulent viscosity.

Kolmes *et al.* (2019) consider the radial currents that are consistent with stationary rotation profiles in the presence of different sources of angular momentum and transverse viscosity. The present paper emphasizes that in open traps, these currents are typically closed by the parallel currents to plasma-facing electrodes (which can be biased.) Thus, the radial currents and the corresponding rotation profiles can be driven by external voltage sources, i.e. by biasing.

† Email address for correspondence: bekl@bk.ru

In this paper, our aim is restricted to a theoretical description of plasma rotation induced by biasing in axially symmetric mirrors. The work is stimulated by extensive experimental data on plasma flow and rotation obtained on the GDT (Bagryansky *et al.* 2015) and SMOLA (Sudnikov *et al.* 2022) devices at the Budker Institute of Nuclear Physics (BINP). Recent experiments on SMOLA (with relatively low plasma temperatures) demonstrated radically different spatial profiles of rotation as compared with earlier experiments on GDT. In particular, in contrast to the radial rotation shear observed and used in the 'vortex confinement' regimes of GDT, the observed plasma rotation in SMOLA is radially rigid but sheared axially. The axial shear, i.e. the gradient of rotation frequency along the trap, is rather difficult to understand in circumstances when the electron temperature is far below the applied biasing potential and thus the electron pressure effects in Ohm's law should be negligible.

To outline the theoretical model and the problem under consideration, we should start with a discussion of terms. The local rotation velocity can be defined as the hydrodynamic mass-flow velocity. In the drift approximation disregarding the electron inertia, it can be decomposed into the drift velocity of ions (including the diamagnetic drift and the guiding centre drift velocities) and the parallel flow rotation (in the presence of an azimuthal magnetic field and parallel plasma flow). Due to the relatively small axial currents in linear traps, in what follows, we can disregard the parallel flow rotation, while the drift velocity of ions satisfies the hydrodynamic equation of ion motion. The two-fluid description is insufficient for plasmas with intense neutral beam heating such as in GDT. In such cases, the two-fluid model should be supplemented with an adequate description of the hot-ion component.

Equations describing the plasma dynamics should be coupled with the corresponding boundary conditions. The term 'biasing' is referring to a specific type of these. Magnetically confined plasma is typically surrounded by various solid surfaces (usually conducting) such as limiters, endplates, vessel walls, etc. Different parts of the plasma-facing surfaces can be grounded, floated or turned into biased electrodes by using external power sources. However, the surface potential is not directly defining the potential of the adjacent plasma due to the Debye shielding. In dense plasmas of fusion traps, the Debye radius is negligible, so that biasing an electrode is meaningful only if there is a possibility of its current connection to the plasma. Then, in a period of time, it may lead to a change in the plasma potential.

As is known from the theory of plane probes (Beilis & Keidar 1998), the spatial structure of the electrostatic potential near the electrode is rather complex: it contains a thin non-neutral 'sheath' and a rather wide quasi-neutral 'presheath' layer. The potential jump in the sheath layer depends on the electron temperature, and the balance of ion and electron currents to the electrode. The structure of the presheath is determined by the distribution of the electron temperature and density along the field lines, and thus by the plasma-flow regime to the electrode. In linear traps, in particular, the distributed potential in expanders can be interpreted as a type of presheath. The parallel electron current is the defining factor in the sheath potential, while its influence on the presheath is negligible unless the electrode is close to the ion-saturation regime. Thus, it can be concluded that the potential difference between the plasma core and the electrodes (outside of saturation regimes) is composed of two parts: the full ambipolar potential, depending on equilibrium parameters of the plasma flow, and the difference between the real and the ambipolar sheath potentials. The second part is affected by the electron current density and thus has very little inertia.

Each open flux tube has two ends on solid surfaces, and thus there are two boundary conditions involving the plasma potential and the current density at boundaries. Flux

https://doi.org/10.1017/S0022377824001454 Published online by Cambridge University Press

tubes can be longer or shorter than the theoretical presheath. In the first case, we can assume that there is some 'core' plasma between boundaries, while the short flux tubes can typically be found between limiters and constitute the scrape-off-layers (SOLs). In the short flux tubes, the plasma content is small since it is due to the balance between cross-field particle transport and particle sources within them, and fast parallel losses to the ends. Low plasma density in the SOL does not mean these discharge areas are unimportant or equivalent to vacuum. They are providing the edge boundary conditions for the core of the plasma column.

To induce the plasma rotation by biasing, it is necessary to propagate the transverse electric fields between the edge electrodes along the field lines into the core plasma. Then the plasma rotation will change due to the resulting radial electric field in it. The transition process is equivalent to an Alfvén wave of twisting propagating from the edge. For transitions slower than the Alfvén transit time, the field-line twisting can be ignored and the process can be described as electrostatic. Electrostatic and electromagnetic cases differ only as to whether there is a parallel inductive electric field along the field lines. In any case, the angular acceleration of the plasma is due to the Ampère force on the radial currents (mainly in ions) which are closed by the parallel electron currents from the electrodes. Alternatively, it can be said that any angular acceleration causes charge-separating radial drift of plasma particles that is neutralized by axial electron currents to the electrodes.

The plasma currents related to its accelerated flow in the magnetic field, especially the fast outflow of rotating plasma in expanders, can alter the weak magnetic fields there. This problem is obviously complex and requires a self-consistent solution. Here, we will assume the magnetic field perturbations to be small.

The plasma inertia requires finite charge to flow from the power source through the sheaths to change the rotation velocity. This process is extended in time and accompanied by energy dissipation at the electrodes. In terms of electric circuits, the sheath structures are similar to thermal voltage sources with nonlinear internal resistance, while the rotating plasma core is equivalent to a capacitor.

Large-area metal endplates were used in early designs of mirrors to provide the line-tying stabilization. The idea is that at low electron temperature (or with unlimited electron emission), the sheath potential and its resistance can be neglected, and then the plasma potential also becomes uniform. The ExB plasma drifts are suppressed. At non-zero temperatures, such electrodes project non-zero radial electric fields into the plasma core due to the radial dependence of the sheath potential and lead to ambipolar plasma rotation. This may become a cause for the temperature-gradient instability of flute modes (Berk, Ryutov & Tsidulko 1991). The sheath resistivity also becomes finite, so that the line-tying just slows the growth rates of flute modes. For modes growing faster than the circuit recharge time, the line-tying fails completely. The sheath resistivity can be reduced by higher emissivity of electrodes but such a set-up effectively limits the electron temperature to a few volts.

The GDT group uses an advanced type of flute-mode suppression called the 'vortex confinement' (Beklemishev *et al.* 2010). The endplates in this case look like relatively biased concentric rings. Alternatively, the biasing voltage can be applied between the central endplates and the limiters. Such arrangement gives rise to a layer of sheared plasma rotation around the flux surface corresponding to the boundary between biased plates. Fast mode rotation plus the sheath dissipation (as in line-tying) lead to nonlinear dissipative saturation of unstable flute modes, somewhat similar to resistive wall stabilization of edge modes in tokamaks. Although both signs of the radial electric field, and thus both rotation directions, are suitable, a better result can be achieved with negative biasing potential

https://doi.org/10.1017/S0022377824001454 Published online by Cambridge University Press

on axis (or with positive potential on limiters). In this case, the induced ExB rotation in GDT discharges is opposite to the ambipolar rotation and the diamagnetic drift, and thus effectively reduces the centrifugal instability drive. Furthermore, the net radial current, driven by the external voltage source, is in ions, and is directed inward, leading to an additional pinch effect.

The discharge in the SMOLA device (Sudnikov *et al.* 2022) is driven by the plasma gun with a heated LaB cathode that covers most of the discharge cross-section. The endplate opposite the cathode is composed of concentric Mo ring electrodes, biased approximately to the cathode potential. The outer concentric anode and limiters can be biased or grounded, while the voltage between the cathode and the outer electrodes can serve to drive the plasma rotation. This set-up is rather generic for the production of rotating plasma discharges. In SMOLA, the high rotation frequency is one of the objectives of the experiment, so that it is measured in detail by spectroscopic means and by Mach probes directly, and via electric field probes indirectly. As mentioned above, the observed results are quite different from those initially expected. Even the scaling of the rotation frequency with the magnetic field is somewhat off. In this paper, we argue that the possible causes of the anomalous structure of rotation are several types of dissipation prominent in SMOLA experiments.

Section 2 presents essential equations for stationary rotating discharges. The physical model is simplified for the description of plasma rotation driven by biasing in GDT-type traps. Section 3 describes the alternative model, relevant for plasmas with high effective viscosity (or discharges with small relative radii). This model emphasizes the role of the plasma–SOL interaction and is intended for interpretation of SMOLA experiments. In § 4, the results are summarized.

2. Standard model of plasma rotation in GDT

Consider the quasi-stationary state of the axially symmetric plasma discharge (on a time scale larger than the Alfvén time). In this case, the electric field can be considered electrostatic and described by means of the local plasma potential distributed on a flux surface ψ along each field line, $\phi = \phi(\psi, z)$. Furthermore, due to the high electron temperature in this model, we will neglect the parallel resistivity of the discharge. Then the parallel electric field within the quasineutral bulk plasma is due entirely to the gradient of the electron pressure. Within the core plasma, the electric field ensures quasineutrality via the Boltzmann distribution of electrons. In the expanders (presheath), the distribution of electrons deviates from the equilibrium, but the potential profiles along a field line, including the non-neutral sheaths, can be calculated (Skovorodin 2019; Chapurin *et al.* 2023).

The scheme of the potential distribution along internal field lines in GDT-type linear traps is presented in figure 1. The potential profile in the quasineutral region, including the core plasma and the expander volume, is essentially determined by the electron temperature and the density distribution, i.e. by the regime of the axial plasma confinement and outflow. As a result, the potential difference $\phi_1 - \phi_2$ is a function of said parameters too. Meanwhile, the sheath potential difference $\Delta S = S_1 - S_2$ depends on the parallel current densities to the endplates, j_1, j_2. Thus, the sheath potentials balance the external $(A_1 - A_2)$ and the internal $(\phi_1 - \phi_2)$ voltages in the presence of the electron currents, making the plasma flow in expanders, in general, non-ambipolar.

The two plasma currents $j_1(S_1)$ and $j_2(S_2)$ have opposite directions due to the orientation of endplates, but let us set their signs the same (as measured by external circuits). Such convention is suitable for relating the currents to the volt–ampère characteristics of sheaths (ignoring their orientation). It is also convenient to measure the parallel current densities

https://doi.org/10.1017/S0022377824001454 Published online by Cambridge University Press

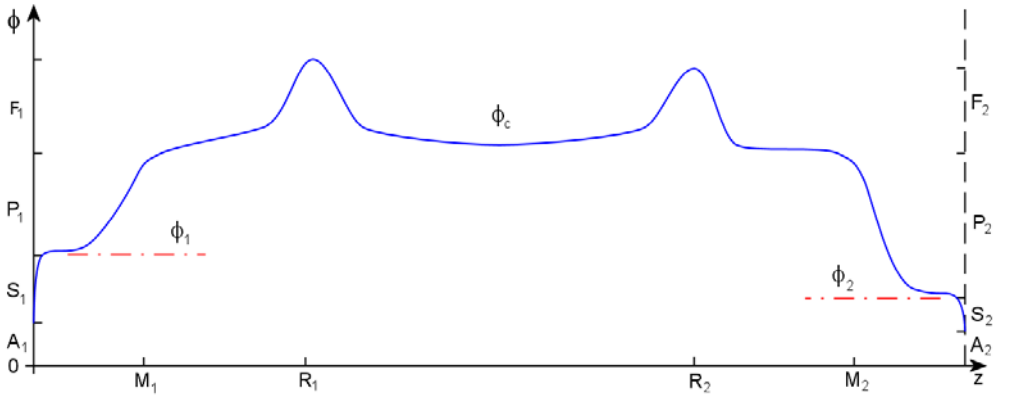

FIGURE 1. Scheme of the potential distribution along a field line in GDT-type linear traps. Subscripts 1, 2 denote values relative to the west and east ends of the device, M_i and R_i are the axial positions of mirror throats and reflection points for sloshing hot ions, respectively, A_i are the voltages applied to the endplates, S_i and P_i are the sheath and presheath (expander) potentials, F_i are the heights of the ambipolar barriers due to the density peaks of hot ions at the reflection points.

per unit flux, i.e. $j_i \equiv \partial I_i/\partial\psi \propto j_\parallel/B$. Then, j_1, j_2 can be rewritten in terms of the 'net' current through the trap $j_n = (j_2 - j_1)/2$ and the 'biasing' current $j_b = j_1 + j_2$ (its closure is by the radial currents). For small currents, in the linear approximation, ΔS will depend only on the net current j_n, but in experiments, the logic is reversed, so j_n is a function of ΔS. For example, the difference in gas conditions and expansion ratio in the east and west ends of the GDT (due to positions of gas puffing and plasma gun placement) results in a significant net axial current (of the order of the ion current) on field lines with $A_1 = A_2$. The net current can be used for 'direct energy conversion', but it results in enhanced energy losses of plasma electrons. Alternatively, the best axial electron confinement can be achieved for the minimum net axial current. This requires application of a suitable external voltage $A_1 - A_2$ between opposite endplates. This is a feedback-type problem since such external voltage depends on plasma conditions and varies in time during the discharge. Alternatively, the endplates can be isolated, but in this case, the ability to set the biasing potential $\phi_b = (A_1 + A_2)/2$ is lost. A rough type of balancing can be achieved by setting a diode circuit on one and the voltage source on the opposite endplate. In the following, we will assume that some kind of balancing is in place, so that the current density to the endplate is less than the ion loss rate, while the functional dependence $j_i(S_i)$ is approximately linear.

To relate figure 1 to the plasma rotation, we need to consider the dependence of shown potentials on the radial position of the field line, i.e. their dependence on the flux coordinate. One part of this functional dependence stems from the radial distribution of electron temperature and plasma density within the discharge, the ambipolar potential $\phi_a(\psi, z)$, the other is due to the radial dependence of the applied biasing voltage on the endplates, $\phi_b(\psi)$, while the third reflects the state of the angular momentum transfer due to radial currents, $\phi_m(\psi)$. The sheath potential S_i contains contributions of the ambipolar and non-ambipolar nature, $S_i = S_{ia} + S_{in}$. This means that the sheath potential is calculated with the assumption of equal electron and ion loss rates, i.e. $j_i = 0$, is S_{ia}. At small currents, $S_i \approx S_{ia} + j_i(\partial S_i/\partial j_i)_a$, $S_{in} \approx j_i(\partial S_i/\partial j_i)_a$. However, both S_{ia}, S_{in} result in z-independent contributions to the overall potential, so that the ambipolar part of the sheath potential can be included either in ϕ_a or in ϕ_m. For the sake of brevity in terms, we will assume that

https://doi.org/10.1017/S0022377824001454 Published online by Cambridge University Press

ϕ_m is non-ambipolar, $\phi_m = (S_{1n} + S_{2n})/2 \propto j_b$, while ϕ_a corresponds to the idealized axial equilibrium with $j_b = 0$ and zero radial currents.

In summary, the plasma potential distribution can be written as a sum of the ambipolar potential, ϕ_a, the biasing potential, ϕ_b, and the non-ambipolar sheath potential, ϕ_m:

$$\phi(\psi, z) = \phi_a(\psi, z) + \phi_b(\psi) + \phi_m(j_b(\psi)). \tag{2.1}$$

In the paraxial approximation, $\mathrm{d}\psi \approx 2\pi r B\,\mathrm{d}r$, so that the ExB drift velocity can be described as

$$v_E = c\frac{-\phi_r'}{B} \approx 2\pi r c\frac{\partial \phi}{\partial \psi}. \tag{2.2}$$

The plasma rotation velocity can be found from the radial component of the equation of motion for the ion fluid (here we again assume a paraxial magnetic structure):

$$-nM\frac{v^2}{r} = -p_r' - qn\varphi_r' + \frac{qn}{c}vB, \tag{2.3}$$

where v is the azimuthal velocity, p_r' is the radial pressure gradient, q is the ion charge and other notation is conventional. As a result,

$$\omega = \frac{v}{r} = \frac{\Omega}{2}\left(\sqrt{1 + 4\frac{v_E}{\Omega r} + \frac{4p_r'}{nM\Omega^2 r}} - 1\right), \tag{2.4}$$

where $\Omega = qB/Mc$ is the ion cyclotron frequency. In the limit of slow rotation, $2\omega/\Omega \ll 1$, when the centrifugal effect is negligible,

$$\omega \approx v_E/r + p_r'/(nM\Omega r) \equiv \omega_E + \omega_d, \tag{2.5}$$

where $\omega_d(\psi, z) = p_r'/(nM\Omega r)$ is the diamagnetic drift frequency of ions. In this limit,

$$\omega(\psi, z) = \omega_d(\psi, z) + 2\pi c\frac{\partial \phi}{\partial \psi} \approx \omega_{da}(\psi, z) + \omega_{bm}(\psi). \tag{2.6}$$

Here, $\omega_{da}(\psi, z) = \omega_d(\psi, z) + 2\pi c(\partial/\partial\psi)\phi_a$ is fully determined by the equilibrium plasma parameters, while $\omega_{bm}(\psi) = 2\pi c(\partial/\partial\psi)(\phi_b + \phi_m)$ is related to biasing and the conservation of the angular momentum. The important point here is that the rotation frequency $\omega_{bm}(\psi)$ is 'rigid' along the field lines (in the presheath and the plasma core), i.e. is constant on each flux surface. In particular, formally increasing the biasing potential far above the plasma temperature, $\omega_{da}(\psi, z) \ll \omega_{bm}(\psi)$, we should get a rigid rotation (along the field lines).

As mentioned above, ϕ_m and ω_{bm} are related to the radial currents, which, in turn, affect the angular velocity. These relationships can be described by the azimuthal component of the fluid equation for the plasma as a whole coupled with the current closure condition on a flux surface:

$$nM\frac{\mathrm{d}v}{\mathrm{d}t} = -\frac{1}{c}j_\psi B + f, \tag{2.7}$$

$$(\boldsymbol{b}\nabla)\frac{j_\parallel}{B} + \frac{\partial}{\partial \psi}\left(2\pi r j_\psi\right) = 0. \tag{2.8}$$

Here, j_ψ is the transverse (radial) current density and f represents the azimuthal non-electromagnetic force per unit volume. In particular, f can stand for the divergence

https://doi.org/10.1017/S0022377824001454 Published online by Cambridge University Press

of the viscous momentum flux, or for the collisional momentum transfer from the beam ions or by charge exchange with neutrals. For simplicity, we again used the paraxial approximation

The radial current density is very difficult to measure experimentally and thus it should be excluded from the system. We find

$$\frac{\partial}{\partial\psi}\left(2\pi r j_\psi\right) = \frac{\partial}{\partial\psi}\frac{2\pi rc}{B}\left(f - nM\frac{\mathrm{d}v}{\mathrm{d}t}\right) = -\left(\boldsymbol{b}\boldsymbol{\nabla}\right)\frac{j_\parallel}{B}, \tag{2.9}$$

$$\frac{\partial}{\partial\psi}\left(\frac{rnM}{B}\frac{\mathrm{d}}{\mathrm{d}t}r\omega\right) = \frac{1}{2\pi c}\left(\boldsymbol{b}\boldsymbol{\nabla}\right)\frac{j_\parallel}{B} + \frac{\partial}{\partial\psi}\left(\frac{rf}{B}\right). \tag{2.10}$$

This equation describes the temporal evolution of the rotation frequency, ω. However, as we found earlier, this frequency comprises two components $\omega = \omega_{da}(\psi, z) + \omega_{bm}(\psi)$, of which the first one is essentially an external parameter, i.e. defined by equations of mass and energy transport outside of this model. Meanwhile, the variable part of the frequency $\omega_{bm}(\psi, t)$ is 'rigid', so that the equation for it can be reduced to the one-dimensional form by averaging along the field lines. After integrating (2.10) along field lines between the opposite endplates, we get

$$\frac{\partial}{\partial\psi}\left(\left\langle\frac{r^2nM}{B}\right\rangle\dot{\omega}_{bm} + U\omega_{bm}\right) = \frac{j_b}{2\pi c} + \frac{\partial}{\partial\psi}\left\langle\frac{r}{B}\left(f - nM\frac{\mathrm{d}}{\mathrm{d}t}r\omega_{da}\right)\right\rangle. \tag{2.11}$$

Here, we assumed that the zero-order approximation $\boldsymbol{v} = v_\parallel\boldsymbol{b} + \boldsymbol{v}_E$ for the advection velocity in the inertial terms is sufficient, took into account that

$$\int\left(\boldsymbol{b}\boldsymbol{\nabla}\right)\frac{j_\parallel}{B}\,\mathrm{d}\ell = \left.\frac{j_\parallel}{B}\right|_{z_1}^{z_2} = j_2 + j_1 = j_b, \tag{2.12}$$

and introduced the notation

$$\langle\,\rangle = \int_{z_1}^{z_2}\mathrm{d}\ell, \quad U(\psi) = \left\langle\frac{rnM}{B}v_\parallel\left(\boldsymbol{b}\boldsymbol{\nabla}\right)r\right\rangle. \tag{2.13a,b}$$

Coefficient U accounts for the angular momentum transfer with the axial plasma flow. Strictly speaking, this is a non-paraxial effect, but it can be important in the case of intense flows in expanders. Namely, taking into account the rigid rotation frequency, the loss rate of the angular momentum with the outflow in expanders will be larger due to the increasing radius of rotation at the endplates.

Equation (2.11) can describe the evolution of $\omega_{bm}(\psi, t)$ if its coefficients and the source terms on the right-hand side are known. However, the line-tying current density j_b depends on the non-ambipolar sheath potential ϕ_m, which contributes to ω_{bm} itself:

$$\omega_{bm} = 2\pi c\frac{\partial}{\partial\psi}\left(\phi_b + \phi_m\right), \tag{2.14}$$

$$j_b = j_b(\phi_m) = j_b\left(\frac{1}{2\pi c}\int\omega_{bm}\,\mathrm{d}\psi - \phi_b\right). \tag{2.15}$$

The explicit form of relation (2.15) depends on the IV characteristic of the sheath layer. For low-emission endplates and low net axial currents (below the ion saturation threshold),

https://doi.org/10.1017/S0022377824001454 Published online by Cambridge University Press

(2.15) can be linearized and rewritten as

$$j_b = j_{\rm ion}\frac{e\phi_m}{T_e} = j_{\rm ion}\frac{e}{T_e}\left(\frac{1}{2\pi c}\int \omega_{bm}\,{\rm d}\psi - \phi_b\right), \tag{2.16}$$

where $j_{\rm ion} = J_i/B$ is the ion current density (per flux tube) to the endplate. In particular, such a model was used earlier by Beklemishev *et al.* (2010).

There is at least one more term on the right-hand side of (2.11) that depends on ω_{bm}. It is the corresponding viscous force

$$f_{\eta b} = \frac{\eta}{r^2}\frac{\partial}{\partial r}\left(r^3\frac{\partial\omega_{bm}}{\partial r}\right), \tag{2.17}$$

where η is the hydrodynamic viscosity. In fusion plasmas, it is usually considered to be very small, but can be anomalous in the presence of turbulence. This term contains the highest radial derivative.

Taking into account the above relations, (2.11) can be rewritten in terms of the plasma potential induced by biasing, $\phi = \phi_b + \phi_m$:

$$\frac{\partial}{\partial\psi}\left(I\frac{\partial\dot\phi}{\partial\psi} + U\frac{\partial\phi}{\partial\psi}\right) - H\,(\phi - \phi_b(\psi)) - \frac{\partial^2}{\partial\psi^2}\left(\Upsilon\frac{\partial^2\phi}{\partial\psi^2}\right) = F, \tag{2.18}$$

where

$$\left.\begin{gathered} I = \left\langle\frac{r^2nM}{B}\right\rangle, \quad F = \frac{\partial}{\partial\psi}\left\langle\frac{r}{2\pi cB}\left(\hat f - nM\frac{\rm d}{{\rm d}t}r\omega_{da}\right)\right\rangle, \\ \Upsilon = 4\pi^2\left\langle\eta Br^4\right\rangle, \quad H = j_{\rm ion}\frac{e}{4\pi^2c^2T_e}, \end{gathered}\right\} \tag{2.19}$$

H corresponds to the sheath-adjacent plasmas and angular brackets denote integration along the field lines. Note that the biasing potential ϕ_b enters through the line-tying term $H(\phi - \phi_b(\psi))$ only.

As an example, let us consider rotation of the plasma column with radially uniform density and electron temperature, driven by biasing adjacent concentric rings of endplates (as in the 'vortex confinement' (Beklemishev 2008; Beklemishev *et al.* 2010)). Then, $\phi_b(\psi)$ is discontinuous like a Heaviside function at $\psi = \psi_0$. Further assume the plasma to be in equilibrium with low axial losses and no momentum injection with beams, $F = 0$, $U = 0$. Then, (2.18) describes how the rotation potential ϕ tries to relax to the applied biasing potential ϕ_b, but is hindered by viscosity. If η is small, the rotation layer in equilibrium is in a small area around ψ_0, and the solution can be found analytically. It was earlier published in Beklemishev (2008) and is shown in figure 2. The main point here is the weak dependence of the solution width Δ around ψ_0 on viscosity

$$\Delta = (\Upsilon/4H)^{1/4}. \tag{2.20}$$

In GDT, the solution width is of the order of 20 % of the plasma radius (by estimates and by probe measurements). If this width were comparable to the discharge radius, we would need to solve the boundary problem and study the boundary conditions for (2.18) (in ψ) in detail.

In summary, the frequency of the plasma rotation in GDT-like devices can be described as having two distinct components: (1) the 'ambipolar' frequency $\omega_{da}(\psi, z)$, which is a function of distributions of density and temperature in the discharge; and (2) the 'driven'

https://doi.org/10.1017/S0022377824001454 Published online by Cambridge University Press

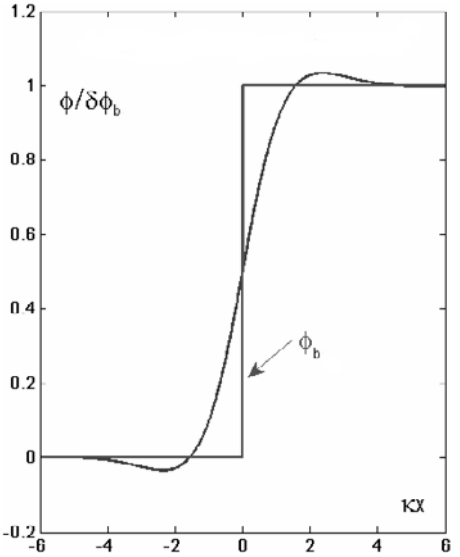

FIGURE 2. Equilibrium profile of the rotation potential driven by biasing adjacent endplates and regularized by viscosity. Here, $x = \psi - \psi_0$, $\kappa = (4H/\Upsilon)^{1/4}$.

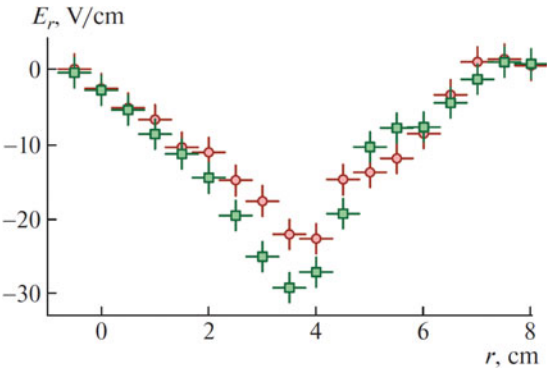

FIGURE 3. Radial distribution of the radial electric field in SMOLA at $Z = 2.04$ m in different magnetic field configurations (Inzhevatkina *et al.* 2024). Approximately linear profile in the plasma core ($r < 3.8$ cm) corresponds to rigid rotation, while in the SOL ($r > 3.8$ cm), the rotation velocity decays to zero.

frequency ω_{bm}, which reflects the radial distribution of the angular momentum. If the axial ion confinement is independent of the 'driven' rotation, then ω_{bm} is constant on each flux surface and its temporal evolution can be found from the equation of the angular momentum transport, (2.18).

3. Rotation of low-temperature plasmas

Plasma rotation in the SMOLA device (Sudnikov *et al.* 2022) exhibits a rigid-rotor type of behaviour in the radius up to the SOL boundary for all types of the biasing distribution. It can be seen from the recently published probe measurements of the radial electric field (Inzhevatkina *et al.* 2024) shown in figure 3.

https://doi.org/10.1017/S0022377824001454 Published online by Cambridge University Press

The radially rigid rotation indicates that, unlike in GDT, the effective viscous transport of momentum in radius is dominant. It should be noted that in these experiments the electron temperature is less than 10 % of the biasing potential, while the diamagnetic drift frequency should also be small. This means that in terms of the previous section, the ambipolar frequency ω_{da} can be neglected. There are also no obvious non-electromagnetic sources of the angular momentum within the discharge core, $\hat{f} = 0$.

As compared with the above GDT-relevant model, the theoretical description of SMOLA discharges should include effects of finite conductivity and fast axial plasma flow. Indeed, the rotation and its potential in SMOLA vary along the discharge. In conjunction with low electron temperature, it means that the parallel gradient of the plasma potential is ohmic. In addition, the plasma gun of SMOLA generates a constant sub-sonic axial flow of plasma through the device. This flow is sure to play an important role in the axial transport of the angular momentum.

Let us construct a simplified model relevant for low-temperature viscous plasmas. Assume that a cylindrical plasma column flows along the uniform magnetic field B and rotates in crossed fields. The ambipolar potential is zero. Assume the rotation to be rigid in radius with frequency $\Omega(z)$ up to the 'edge' at $r = a$ (in the SOL, at $r > a$, the rotation is no longer rigid.) Assumption of the rigid rotor replaces the equation of the momentum transport in radius, while the feature of the model will be construction of the equation for the axial transport of the angular momentum.

For a rigid $E \times B$ rotation, the plasma potential is parabolic ($v(r) \propto r$ and the edge potential is $\phi(a) = \varphi_*(z)$):

$$\phi(r, z) = \frac{B}{2c}\Omega(z)\left(r^2 - a^2\right) + \varphi_*(z). \tag{3.1}$$

The axial plasma current density can then be found from Ohm's law:

$$j_z(r, z) = \sigma E_z = \frac{\sigma B}{2c}\Omega'(z)\left(a^2 - r^2\right) - \sigma\varphi_*'(z). \tag{3.2}$$

The radial current density can be found from the current closure condition. In the case of radially uniform conductivity $\sigma(r) = const.$, it is also parabolic:

$$j_r(r, z) = -\frac{1}{r}\int_0^r \frac{\partial j_z}{\partial z} r\,\mathrm{d}r = \sigma\frac{Br}{8c}\Omega''(z)\left(r^2 - 2a^2\right) + \sigma\frac{r}{2}\varphi_*''(z). \tag{3.3}$$

In our model, there are two possible sources of torque: Ampère's force, $j_r B_z$, and the edge friction. Then the balance of the angular momentum looks like

$$\frac{\partial\Phi(z)}{\partial z} = M_A + M_\eta. \tag{3.4}$$

Here, Φ is the axial flux of the angular momentum,

$$\Phi(z) = 2\pi\Omega(z)\int_0^a \rho v_z r^3\,\mathrm{d}r \equiv G\Omega, \tag{3.5}$$

$$M_A = -\frac{2\pi}{c}\int_0^a j_r B r^2\,\mathrm{d}r = \frac{\pi\sigma B^2}{12c^2}a^6\Omega''(z) - \frac{\pi\sigma B}{4c}a^4\varphi_*''(z) \tag{3.6}$$

is the torque of Ampère's force, while the torque of the edge friction, M_η, should be found from the boundary conditions in radius.

https://doi.org/10.1017/S0022377824001454 Published online by Cambridge University Press

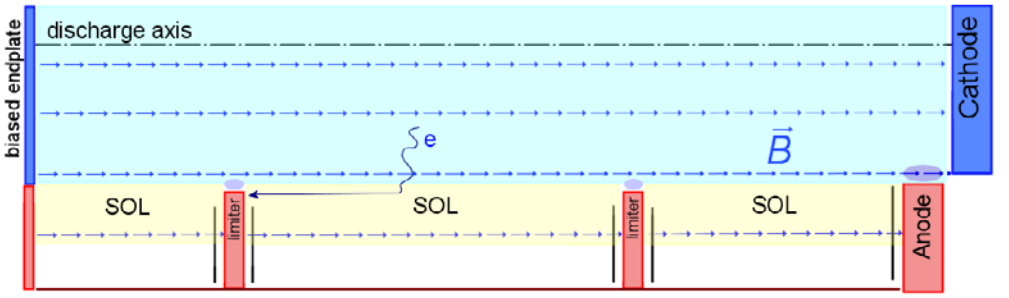

FIGURE 4. Scheme of the structure and the boundary conditions of the model discharge.

The structure of the model discharge as well as the realistic boundaries are shown in figure 4. Along the magnetic field $\boldsymbol{B}$, the discharge is in electrical contact with the cathode and the biased endplate. There is a plasma source at the cathode and a sink at the endplate. At $r = a$, the discharge is in contact with the SOL plasma. The SOL plasma is in contact with the anode, limiters and floating shielding. Some current may flow to the inner faces of the anode and limiters, or to their sides across the SOL.

In general, areas on top of limiters are rather small and should not exert too much of an influence on plasma dynamics (though this may not be the case for the anode). These areas should exhibit the sheath property of shielding the external electric potential of nearby electrodes by higher density of electrons. However, the radial current density there should be in electrons mostly (in the absence of surface ion sources) and thus be small, unless there is a significant azimuthal friction force on electrons. Such a force can be due to the neutral gas atoms or the plasma ions. Both these contributing forces should be present on the SOL boundary away from the limiters as well. The SOL boundary has a much larger area than the limiter tops, so that the radial current flows mostly through this boundary and then to the sides of the limiters. The anode top may be different due to higher gas density there and its higher area in some trap designs.

Discussing the role of limiters, it should also be noted that their side surfaces act as electrodes with line-tying properties, i.e. provide an effective friction for the plasma rotation due to the sheath dissipation. This friction in principle can be mitigated by splitting the side surfaces into radially isolated rings. Biasing the limiters should be effective only if the plasma density in the SOL is sufficiently high, since the biasing current is limited by the ion current from the SOL to the limiter side. Shielding the sides of a limiter by floating electrodes reduces the biasing current limit and ultimately becomes equivalent to setting the whole limiter at the floating potential.

The SOL plasma experiences azimuthal radially differential flow, while the axial flow can be neglected. Then, in the slab approximation (the SOL width is usually smaller than its radius):

$$\frac{\partial \Pi_{xy}}{\partial x} = -\frac{1}{c} j_x B - q v_y, \quad \Pi_{xy} = \rho v_x v_y - \eta \frac{\partial v_y}{\partial x}, \tag{3.7a,b}$$

where x is in the radial and y is in the azimuthal directions, Π_{xy} is the radial flux of the azimuthal momentum and qv_y is the momentum transfer to neutrals. Thus, the radial flux of momentum in the SOL can decay either due to Ampère's force via currents to the limiters, or by recycling.

https://doi.org/10.1017/S0022377824001454 Published online by Cambridge University Press

Using again the current closure and Ohm's law,

$$\frac{\partial j_x}{\partial x} = -\frac{\partial j_z}{\partial z} = \sigma_s \frac{\partial^2 \phi}{\partial z^2}, \tag{3.8}$$

and in terms of the electrostatic potential, we get ($\rho v_x \to 0$, $v_y = c/B(\partial\varphi/\partial x)$):

$$\left(\frac{B^2\sigma_s}{c^2}\right)\frac{\partial^2\phi}{\partial z^2} = \eta\frac{\partial^4\phi}{\partial x^4} - q\frac{\partial^2\phi}{\partial x^2}. \tag{3.9}$$

Though (3.9) is comprehensive, it is too complicated to use, especially since the plasma parameters in the SOL are usually known rather poorly.

Consider the line-tying regime in the SOL: neglect recycling ($q = 0$), integrate between limiters (L_m is the line length) and apply boundary conditions on them ($j_z = \pm J_{\rm lim}$):

$$\frac{\partial^4\phi}{\partial x^4} = \frac{2B^2 J_{\rm lim}}{\eta c^2 L_m}. \tag{3.10}$$

Assuming that the limiters are biased to a fixed potential $\phi_{\rm lim}$ and the sheath current density is far from saturation, the current density to the limiters is

$$J_{\rm lim} \approx J_i\,(1 - \exp\left(e(\phi_{\rm lim} - \phi)/T_e\right)) \approx eJ_i/T_e\,(\phi - \phi_{\rm lim})\,, \tag{3.11}$$

where J_i is the ion flux density. Then,

$$d_\eta^4\phi'''' + \phi - \phi_{\rm lim} = 0, \tag{3.12}$$

with the characteristic radial SOL width

$$d_\eta = \left(\frac{\eta c^2 L_m T_e}{2J_i e B^2}\right)^{1/4}. \tag{3.13}$$

This width can be estimated for SMOLA parameters as $d_\eta \sim 0.6$ cm (with the classic viscosity η Braginskii 1965). However, this estimate is not really reliable and can be regarded as a rough lower limit. In the presence of turbulence, η and d_η should be larger, while the turbulence is in fact observed at the SOL boundary. Another possible cause for the increase in d_η is the saturation of the electron sheath current. It occurs due to the fact that the transverse current is mostly in ions, while the non-ambipolar current to the limiters is in electrons. Thus, the number of electrons that can be extracted from each flux tube is limited. In other terms, the presheath length can become larger than L_m. In this case, the line-tying effect weakens and the SOL width is enhanced.

Another possible plasma behaviour in the SOL can be denoted as the recycling regime: neglect Ampère's force (the left-hand side) in (3.9), then it yields

$$\phi''' - \frac{q}{\eta}\phi' = 0, \quad \phi = (\varphi_* - \varphi_0)\exp\left(-x/d_q\right) + \varphi_0, \tag{3.14}$$

where $d_q = \sqrt{\eta/q}$ and φ_0 is the potential of the outer shell. For SMOLA, $d_q \sim 0.3{-}3$ cm, depending on estimates of viscosity and the density of neutrals, which is comparable to d_η. This means that both the recycling and the line-tying can play a role.

https://doi.org/10.1017/S0022377824001454 Published online by Cambridge University Press

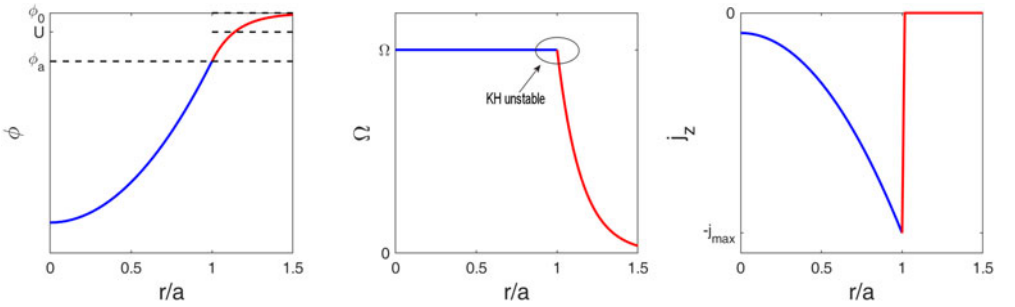

FIGURE 5. Matching the discharge core ($r < a$) and the SOL layer.

The matching conditions for the plasma core to the boundary of the SOL are as follows: the potential ϕ is continuous,

$$\Omega = \frac{v_y(a)}{a} = \frac{c}{aB}\left.\frac{\partial\phi}{\partial x}\right|_a, \tag{3.15}$$

$$M_v = 2\pi a^2 \eta \left.\frac{\partial v_y}{\partial x}\right|_a \tag{3.16}$$

and $j_\perp(a) = j_x$. The last condition (of the current continuity) is relevant for the line-tying regimes in the SOL, while in the recycling regime the current density plays no role in the plasma dynamics.

It is very difficult to measure the transport coefficients in the SOL to evaluate the matching conditions. However, the problem can be reversed: we can obtain information about conditions in the SOL by measuring the radial profile of potential there. Assume that we can measure the gradient length d of the radial electric field at the inner edge of the SOL ($\partial v_y/\partial x|_a = -(a\Omega/d)$) and the asymptotic value of the electrostatic potential at the outer edge of the SOL, φ_0. Then the matching conditions are

$$M_v = -2\pi a^3 \frac{\eta}{d}\Omega, \tag{3.17}$$

and, assuming an approximately exponential profile of ϕ (like in the recycling regime of the SOL),

$$\varphi_* \approx \varphi_0 - \frac{Bda}{c}\Omega. \tag{3.18}$$

The effective viscosity, η, is also difficult to measure. However, it can be found from the value of M_v via measurements of $\Omega(z)$ profiles. This relationship is discussed below.

The scheme of matching the rigidly rotating discharge core to the SOL is shown in figure 5. The $\Omega(r)$ profile in the matching zone $r \approx a$ satisfies the necessary condition for the Kelvin–Helmholtz instability. Indeed, its smoothed version contains the inflection point. In SMOLA, the core edge appears to be the source of fluctuations (Tolkachev *et al.* 2024). As a result, viscosity and resistivity there are likely anomalous. As shown in the graph for the axial current density, j_z, its absolute value in the edge zone is enhanced, while the axial ohmic field can cause the axial dependence of $\varphi_*(z) = \phi(a, z)$ and hence, $\Omega(z)$.

https://doi.org/10.1017/S0022377824001454 Published online by Cambridge University Press

Axial dependence of Ω can be deduced from the torque balance equation, $\partial\Phi(z)/\partial z = M_A + M_v$. Using the 'experimental' matching conditions, in terms of $\Omega(z)$, it looks as

$$\frac{\pi\sigma B^2}{12c^2}a^5(a+d)\frac{\partial^2\Omega}{\partial z^2} - \frac{\partial}{\partial z}(G\Omega) - \frac{2\pi a^3}{d}\eta\Omega = \frac{\pi\sigma B}{4c}a^4\varphi_0''(z). \tag{3.19}$$

The physical meaning of the equation terms here is as follows.

(i) The torque via Ampère's force due to the biasing of end electrodes. In ideally conducting plasma ($\sigma \to \infty$), it is dominant and ensures $\Omega = \text{const.}$ in z.
(ii) The divergence of the axial flow of the angular momentum with the plasma flow ensures its continuity.
(iii) The frictional torque caused by interaction with the SOL plasma at the core edge.
(iv) The effect of the axially distributed SOL biasing, if present (via the limiters in the line-tying regime or via the conducting shell).

The above equation for $\Omega(z)$ can be rewritten in the normalized form as

$$L^2\frac{\partial^2\Omega}{\partial z^2} - \Omega = \frac{\partial}{\partial z}\left(\hat{G}\Omega\right) + D. \tag{3.20}$$

Here, L is the characteristic axial variation length,

$$L = c_A\sqrt{\tau_\sigma\tau_\eta/24} \propto Ba^{3/2}\sigma^{1/2}\eta^{-1/4}, \tag{3.21}$$

where c_A is the Alfvén velocity, τ_σ is the resistive time and τ_η is the viscous momentum transport time:

$$\tau_\sigma = \frac{4\pi\sigma}{c^2}a^2, \quad \tau_\eta = \frac{\rho d(a+d)}{\eta}, \tag{3.22a,b}$$

$$\hat{G} = \int_0^1 v_z\tau_\eta\left(\frac{\rho r^3}{\rho_* a^3}\right)\mathrm{d}\left(\frac{r}{a}\right) \tag{3.23}$$

is the normalized axial plasma flux and

$$D = \frac{\sigma Bad}{8c\eta}\varphi_0''(z). \tag{3.24}$$

Equation (3.20) can be solved with suitable boundary conditions (modelling the cathode and the endplates) along the discharge, if its coefficients are defined. Unfortunately, they are not, as it is very difficult to measure or calculate the anomalous plasma viscosity. In these circumstances, it would be more effective to use (3.20) to find L and then η via measurements of $\Omega(z)$.

The axial distribution of the electric field depends on the plasma resistivity as well. It is easier to measure than the viscosity, but there may exist another complication. Namely, Ohm's law for discharges with emissive cathodes (like in SMOLA) may need modification to include the electron inertia. Indeed, the parabolic form of the plasma potential in the radius suggests that the sheath potential at the cathode edge in the radius may be large, of the order of the full biasing potential. Then, at least part of the axial electron current may be sustained by the beam effect, which is not included in the present model.

https://doi.org/10.1017/S0022377824001454 Published online by Cambridge University Press

4. Conclusion

We presented two theoretical models of the plasma rotation induced by biasing in axially symmetric traps. The difference between these models is in the role of the effective plasma viscosity that describes the radial transport of the angular momentum.

For fusion-relevant plasma parameters, the rotation driven by biasing or by external sources of momentum can be described as axially rigid. It is superimposed by the non-rigid rotation due to the ambipolar plasma potential, defined by the equilibrium plasma distribution. The radial structure of the driven rotation is complicated, its temporal evolution depends on the biasing geometry as well as the transport of the angular momentum.

In low-temperature or small-radius discharges (such as in SMOLA), the viscosity can cause the plasma rotation to be radially rigid, while in the presence of finite parallel conductivity, the rotation frequency may vary along the device. In this model, the loss of angular momentum is due to friction with the SOL plasma at the edge. The axial decay length of the rotation frequency is $L = c_A\sqrt{\tau_\sigma \tau_\eta/24}$. The area of contact of the core plasma with the SOL may be turbulent (this increases the effective viscosity) due to the Kelvin–Helmholtz instability. Faster rotation of the core can be achieved by increasing the magnetic field, by lowering the effective viscosity and by suppressing the momentum loss rate in the SOL. The latter requires lowering the recycling rate and using limiter designs that prohibit radial currents to reduce the line-tying effects.

Biasing the plasma-facing electrodes remains the simplest and cost-effective means to drive the plasma rotation in linear traps. It is less obvious that improvement of the plasma parameters makes it more, rather than less, efficient since the necessary biasing currents drop. Estimates by Skovorodin *et al.* (2023) show that the biasing-based 'vortex confinement' can be realized in the next-generation fusion trap, GDMT.

Acknowledgements

The author is grateful to the experimental groups of GDT and SMOLA traps in the Budker INP, especially to A. Sudnikov, A. Inzhevatkina and E. Soldatkina for providing and discussing the relevant experimental data.

Editor C. Forest thanks the referees for their advice in evaluating this article.

Funding

This work was supported by Russian Science Foundation Grant no. 22-12-00133.

Declaration of interests

The author reports no conflict of interest.

REFERENCES

Bagryansky, P., Anikeev, A., Denisov, G., Gospodchikov, E., Ivanov, A., Lizunov, A., Kovalenko, Y., Malygin, V., Maximov, V., Korobeinikova, O., *et al*. 2015 Overview of ECR plasma heating experiment in the GDT magnetic mirror. *Nucl. Fusion* **55** (5), 053009.

Beilis, I.I. & Keidar, M. 1998 Sheath and presheath structure in the plasma–wall transition layer in an oblique magnetic field. *Phys. Plasmas* **5** (5), 1545–1553.

Beklemishev, A.D. 2008 Shear-flow effects in open traps. *AIP Conf. Proc*. **1069** (1), 3–14.

Beklemishev, A.D., Bagryansky, P.A., Chaschin, M.S. & Soldatkina, E. 2010 Vortex confinement of plasmas in symmetric mirror traps. *Fusion Sci. Technol*. **57**, 351–360.

Berk, H.L., Ryutov, D.D. & Tsidulko, Y.A. 1991 Temperature-gradient instability induced by conducting end walls. *Phys. Fluids* B **3** (6), 1346–1354.

https://doi.org/10.1017/S0022377824001454 Published online by Cambridge University Press

BRAGINSKII, S.I. 1965 Transport processes in a plasma. *Rev. Plasma Phys*. **1**, 205.

CHAPURIN, O., JIMENEZ, M., SMOLYAKOV, A., YUSHMANOV, P. & DETTRICK, S. 2023 Plasma flow and instabilities in the magnetic mirror with ion recycling and neutral back-flow. *Phys. Plasmas* **30** (11), 112510.

INZHEVATKINA, A.A., IVANOV, I.A., POSTUPAEV, V.V., SUDNIKOV, A.V., TOLKACHEV, M.S. & USTYUZHANIN, V.O. 2024 Investigation of plasma flow velocity in the helical magnetic open trap SMOLA. *Plasma Phys. Rep*. **50** (1), 1–11.

KOLMES, E.J., OCHS, I.E., MLODIK, M.E., RAX, J.-M., GUEROULT, R. & FISCH, N.J. 2019 Radial current and rotation profile tailoring in highly ionized linear plasma devices. *Phys. Plasmas* **26** (8), 082309.

SKOVORODIN, D.I. 2019 Influence of trapped electrons on the plasma potential in the expander of an open trap. *Plasma Phys. Rep*. **45** (9), 799–804.

SKOVORODIN, D.I., CHERNOSHTANOV, I.S., AMIROV, V.K., ASTRELIN, V.T., BAGRYANSKII, P.A., BEKLEMISHEV, A.D., BURDAKOV, A.V., GORBOVSKII, A.I., KOTEL'NIKOV, I.A., MAGOMMEDOV, E.M., *et al*. 2023 Gas-dynamic multiple-mirror trap GDMT. *Plasma Phys. Rep*. **49**, 1039–1086.

SUDNIKOV, A.V., IVANOV, I.A., INZHEVATKINA, A.A., LARICHKIN, M.V., POSTUPAEV, V.V., SKLYAROV, V.F., TOLKACHEV, M.S. & USTYUZHANIN, V.O. 2022 Helical magnetic mirror performance at up- and downstream directions of the axial force. *J. Plasma Phys*. **88** (6), 905880609.

TOLKACHEV, M.S., INZHEVATKINA, A.A., SUDNIKOV, A.V. & CHERNOSHTANOV, I.S. 2024 Electromagnetic oscillations and anomalous ion scattering in the helically symmetric multiple-mirror trap. *J. Plasma Phys*. **90**, 975900102.

https://doi.org/10.1017/S0022377824001454 Published online by Cambridge University Press